Magnetism -2

Ferromagnetic domains

- Competition between exchange, anisotropy, and magnetic energies.
- Bloch wall: rotation out of the plane of the two spins
- Neel wall: rotation within the plane of the two spins

For a 180° Bloch wall rotated in N+1 atomic planes $N\Delta E_{ex} = N(JS^2\left(\frac{\pi}{N}\right)^2)$

Wall energy density $\sigma_w = \sigma_{ex} + \sigma_{anis} \approx JS^2\pi^2/(Na^2) + KNa$ a : lattice constant

$\partial\sigma_w/\partial N \equiv 0,$ $N = \sqrt{[JS^2\pi^2/(Ka^3)]} \approx 300$ in Fe

$\sigma_w = 2\pi\sqrt{KJS^2/a} \approx$ 1 erg/cm^2 in Fe

Wall width $Na = \pi\sqrt{JS^2/Ka} \equiv \pi\sqrt{\frac{A}{K}}$, $A = JS^2/a$ Exchange stiffness constant

Domain wall energy γ vs thickness D of $Ni_{80}Fe_{20}$ thin films

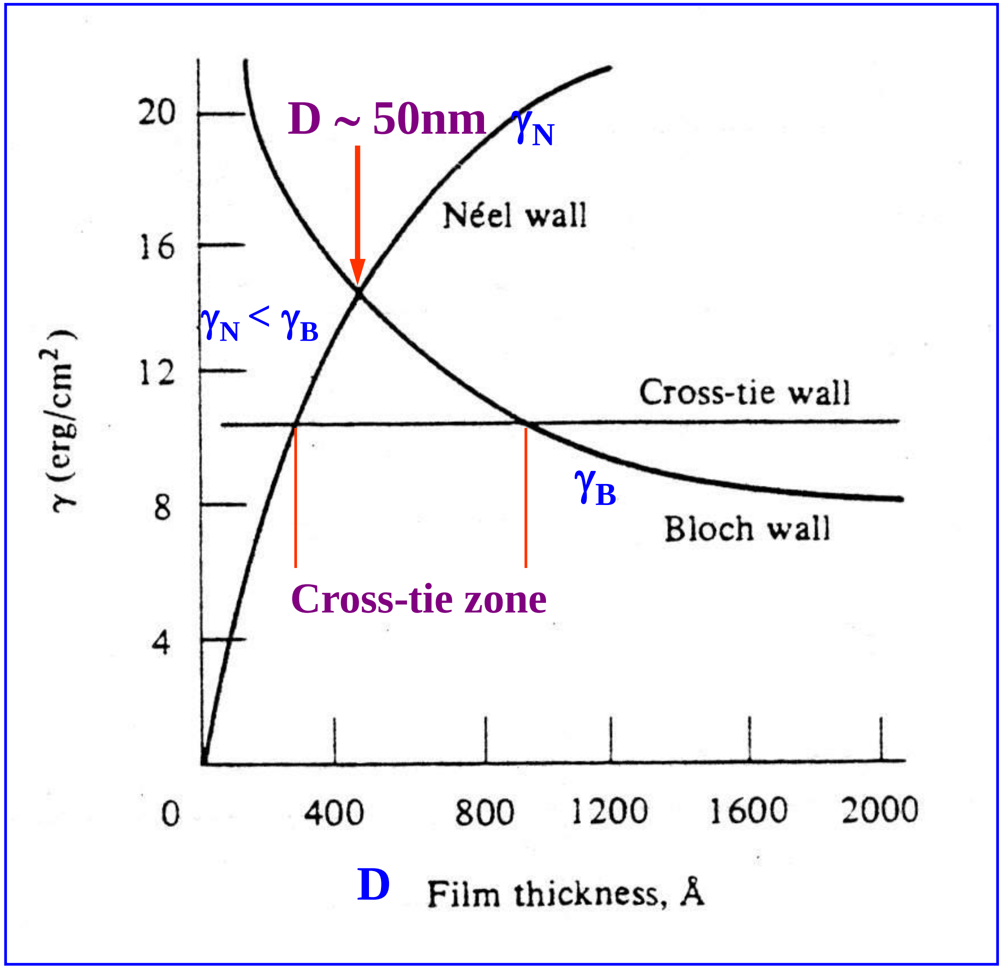

$\gamma_N < \gamma_B$ ~ 50nm

- Thick films have Bloch walls
- Thin films have Neel walls
- Cross-tie walls show up in between.
- $A = 10^{-6}$ erg/cm
- $K = 1500$ erg/cm^3

Magnetic Resonance

- Nuclear Magnetic Resonance (NMR)
  - Line width
  - Hyperfine Splitting, Knight Shift
  - Nuclear Quadrupole Resonance (NQR)
- Ferromagnetic Resonance (FMR)
  - Shape Effect
  - Spin Wave resonance (SWR)
- Antiferromagnetic Resonance (AFMR)
- Electron Paramagnetic Resonance (EPR or ESR)
  - Exchange narrowing
  - Zero-field Splitting
- Maser

What we can learn:

- From absorption fine structure → electronic structure of single defects
- From changes in line width → relative motion of the spin to the surroundings
- From resonance frequency → internal magnetic field
- Collective spin excitations

FMR

Equation of motion of a magnetic moment $\boldsymbol{\mu}$ in an external field B_0

$$\frac{\hbar d\boldsymbol{I}}{dt} = \boldsymbol{\mu} \times \boldsymbol{B} \qquad \boldsymbol{\mu} = \gamma\hbar\boldsymbol{I} \qquad \frac{d\boldsymbol{\mu}}{dt} = \gamma\boldsymbol{\mu} \times \boldsymbol{B} \qquad \frac{d\boldsymbol{M}}{dt} = \gamma\boldsymbol{M} \times \boldsymbol{B}$$

Shape effect:

internal magnetic field

Landau-Lifshitz-Gilbert (LLG) equation

$$\frac{d\boldsymbol{M}}{dt} = -\gamma\boldsymbol{M} \times \boldsymbol{H}_{\mathrm{eff}} + \alpha\boldsymbol{M} \times \frac{d\boldsymbol{M}}{dt}$$

$$B_x^i = B_x^0 - N_x M_x \qquad B_y^i = B_y^0 - N_y M_y \qquad B_z^i = B_z^0 - N_z M_z$$

$$\frac{dM_x}{dt} = \gamma\left(M_y B_z^i - M_z B_y^i\right) = \gamma\left[B_0 + \left(N_y - N_z\right)M\right]M_y$$

$$\frac{dM_y}{dt} = \gamma[M(-N_x M_x) - M_x(B_0 - N_z M)] = -\gamma[B_0 + (N_x - N_z)M]M_x$$

To first order $\quad \dfrac{dM_z}{dt} = 0 \qquad M_z = M$

$$\begin{vmatrix} i\omega & \gamma\left[B_0 + \left(N_y - N_z\right)M\right] \\ -\gamma[B_0 + (N_x - N_z)M] & i\omega \end{vmatrix} = 0$$

$$\omega_0^2 = \gamma^2\left[B_0 + \left(N_y - N_z\right)M\right][B_0 + (N_x - N_z)M]$$

Uniform mode

Uniform mode

Sphere

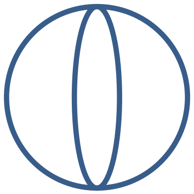

$N_x = N_y = N_z$

$\omega_0 = \gamma\, B_0$

flat plate with perpendicular field

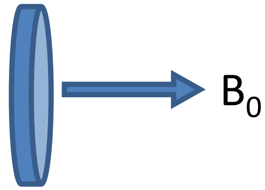

$N_x = N_y = 0 \qquad N_z = 4\pi$

$\omega_0 = \gamma\,(B_0 - 4\pi M)$

flat plate with in-plane field

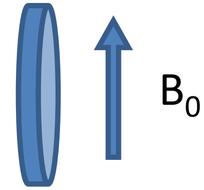

$N_x = N_z = 0 \qquad N_y = 4\pi$

$\omega_0 = \gamma\,[B_0(B_0 + 4\pi M)]^{1/2}$

Spin wave resonance, Magnons

Consider a one-dimensional spin chain with only nearest-neighbor interactions.

$U = -2J \sum \vec{S_i} \cdot \vec{S_j}$ We can derive $\hbar\omega = 4JS(1 - \cos ka)$

When *ka* << 1 $\hbar\omega \cong (2JSa^2)k^2$

flat plate with perpendicular field $\omega_0 = \gamma\,(B_0 - 4\pi M) + Dk^2$

Quantization of (uniform mode) spin waves, then consider the thermal excitation of Mannons, leads to Bloch $T^{3/2}$ law. $\Delta M/M(0) \propto T^{3/2}$

AFMR

Spin wave resonance, Antiferromagnetic Magnons

Consider a one-dimensional antiferromangetic spin chain with only nearest-neighbor interactions. Treat sublattice A with up spin S and sublattice B with down spin –S, J<0.

$U = -2J \sum \vec{S_i} \cdot \vec{S_j}$ We can derive $\hbar\omega = -4JS|\sin ka|$

When *ka* << 1 $\hbar\omega \cong (-4JS)|ka|$

AFMR

exchange plus anisotropy fields on the two sublattices

$\boldsymbol{B}_1 = -\lambda \boldsymbol{M}_2 + B_A \hat{\boldsymbol{z}}$ on $\mathbf{M}_1$ $\boldsymbol{B}_2 = -\lambda \boldsymbol{M}_1 - B_A \hat{\boldsymbol{z}}$ on $\mathbf{M}_2$

$M_1^z \equiv M$ $M_2^z \equiv -M$ $M_1^+ \equiv M_1^x + iM_1^y$ $M_2^+ \equiv M_2^x + iM_2^y$ $B_E \equiv \lambda M$

$$\frac{dM_1^+}{dt} = -i\gamma[M_1^+(B_A + B_E) + M_2^+ B_E]$$

$$\frac{dM_2^+}{dt} = -i\gamma[M_2^+(B_A + B_E) + M_1^+ B_E]$$

$$\begin{vmatrix} \gamma(B_A + B_E) - \omega & \gamma B_E \\ B_E & \gamma(B_A + B_E) + \omega \end{vmatrix} = 0$$

$\omega_0^2 = \gamma^2 B_A(B_A + 2B_E)$ Uniform mode

Spintronics

Electronics with electron spin as an extra degree of freedom
Generate, inject, process, and detect spin currents

- Generation: ferromagnetic materials, spin Hall effect, spin pumping effect etc.
- Injection: interfaces, heterogeneous structures, tunnel junctions
- Process: spin transfer torque
- Detection: Giant Magnetoresistance, Tunneling MR
- Historically, from magnetic coupling to transport phenomena
- Important materials: CoFe, CoFeB, Cu, Ru, IrMn, PtMn, MgO, Al_2O_3, Pt, Ta.

RKKY (*Ruderman-Kittel-Kasuya-Yosida*) interaction

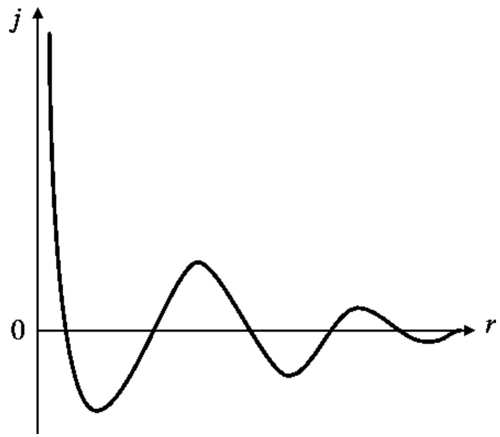

coupling coefficient

$$j\left(\boldsymbol{R}_l - \boldsymbol{R}_{l'}\right) = 9\pi\left(\frac{j^2}{\epsilon_F}\right) F\left(2k_F|\boldsymbol{R}_l - \boldsymbol{R}_{l'}|\right)$$

$$F(x) = \frac{x\cos x - \sin x}{x^4}$$

Magnetic coupling in superlattices

- Long-range incommensurate magnetic order in a Dy-Y multilayer

M. B. Salamon, Shantanu Sinha, J. J. Rhyne, J. E. Cunningham, Ross W. Erwin, Julie Borchers, and C. P. Flynn, Phys. Rev. Lett. **56**, 259 - 262 (1986)

- Observation of a Magnetic Antiphase Domain Structure with Long- Range Order in a Synthetic Gd-Y Superlattice

C. F. Majkrzak, J. W. Cable, J. Kwo, M. Hong, D. B. McWhan, Y. Yafet, and J. V. Waszczak,C. Vettier, Phys. Rev. Lett. **56**, 2700 - 2703 (1986)

- Layered Magnetic Structures: Evidence for Antiferromagnetic Coupling of Fe Layers across Cr Interlayers

P. Grünberg, R. Schreiber, Y. Pang, M. B. Brodsky, and H. Sowers, Phys. Rev. Lett. **57**, 2442 - 2445 (1986)

Magnetic coupling in multilayers

- Long-range incommensurate magnetic order in a Dy-Y multilayer

M. B. Salamon, Shantanu Sinha, J. J. Rhyne, J. E. Cunningham, Ross W. Erwin, Julie Borchers, and C. P. Flynn, Phys. Rev. Lett. 56, 259 (1986)

- Observation of a Magnetic Antiphase Domain Structure with Long-Range Order in a Synthetic Gd-Y Superlattice

C. F. Majkrzak, J. W. Cable, J. Kwo, M. Hong, D. B. McWhan, Y. Yafet, and J. V. Waszczak,C. Vettier, Phys. Rev. Lett. 56, 2700 (1986)

- Layered Magnetic Structures: Evidence for Antiferromagnetic Coupling of Fe Layers across Cr Interlayers

P. Grünberg, R. Schreiber, Y. Pang, M. B. Brodsky, and H. Sowers, Phys. Rev. Lett. 57, 2442 (1986)

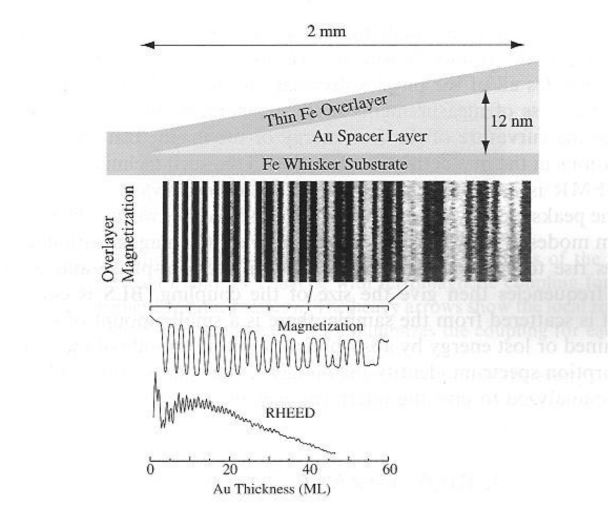

Coupling in a wedge-shape,

Fe/Cr/Fe

Fe/Au/Fe

Fe/Ag/Fe

J. Unguris, R. J. Celotta, and D. T. Pierce

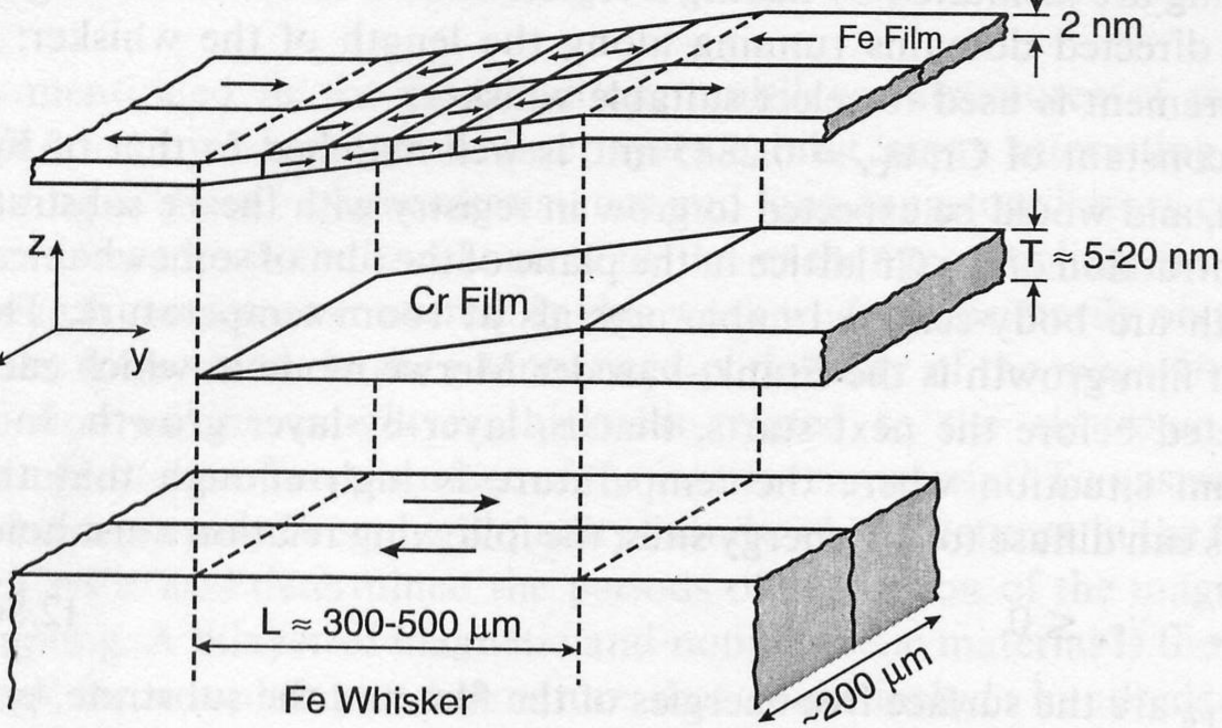

Fig. 2.41. A schematic expanded view of the sample structure showing the Fe(0 0 1) single-crystal whisker substrate, the evaporated Cr wedge, and the Fe overlayer. The arrows in the Fe show the magnetization direction in each domain. The z-scale is expanded approximately 5000 times. (From [2.206])

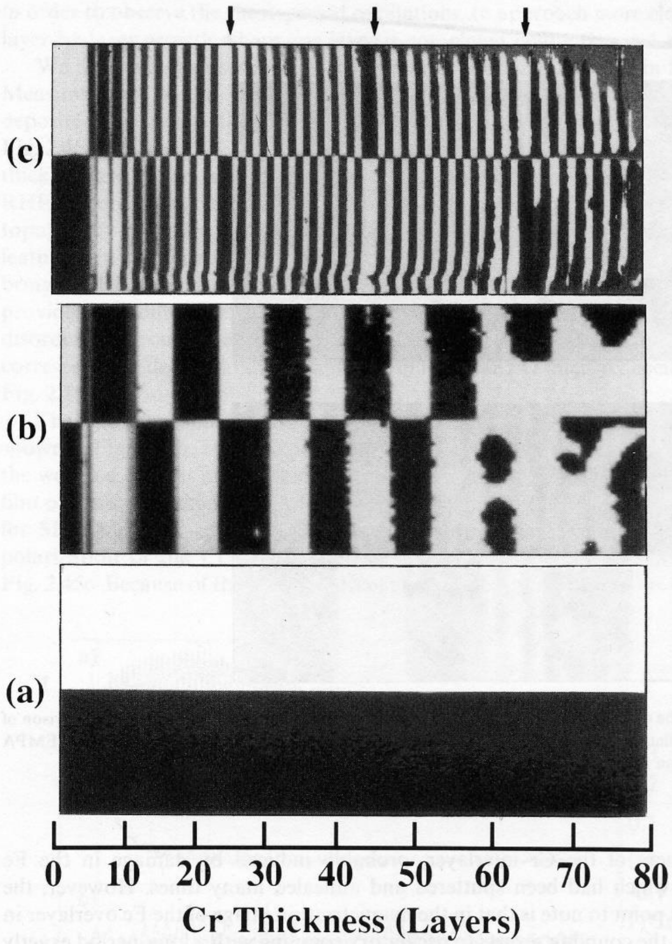

Fig. 2.43. SEMPA image of the magnetization M_y (axes as in Fig. 2.41) showing domains in (**a**) the clean Fe whisker, (**b**) the Fe layer covering the Cr spacer layer evaporated at 30 °C, and (**c**) the Fe layer covering a Cr spacer evaporated on the Fe whisker held at 350 °C. The scale at the bottom shows the increase in the thickness of the Cr wedge in (**b**) and (**c**). The arrows at the top of (**c**) indicate the Cr thicknesses where there are phase slips. The region of the whisker imaged is about 0.5 mm long

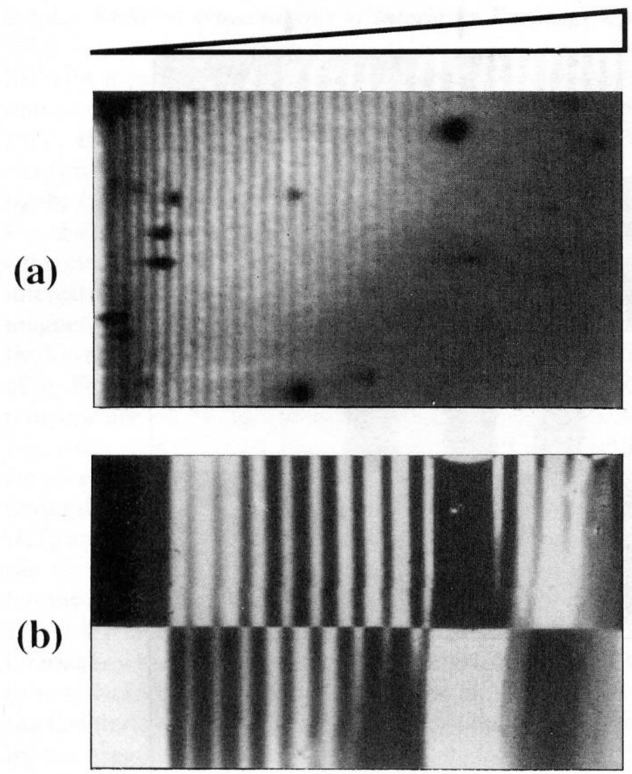

Fig. 2.44. The effect of roughness on the inertlayer exchange coupling is shown by a comparison of (**a**) the oscillations of the RHEED intensity along the bare Cr wedge with (**b**) the SEMPA magnetization image over the same part of the wedge

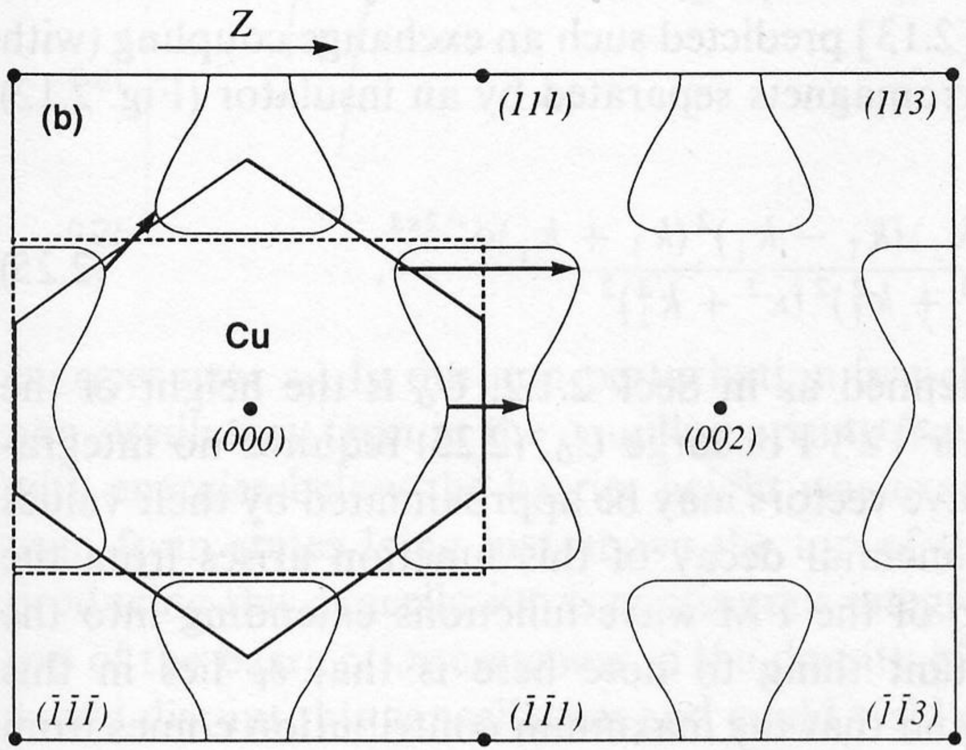

Fig. 2.11. Fermi surface of Cu in the (1 0 0) plane in the extended zone scheme. Arrows indicate values of $2(k_F - G)$ for reciprocal lattice vectors G which can give rise to oscillations with periods greater than π/k_F

Oscillatory magnetic coupling in multilayers

Ru interlayer has the largest coupling strength

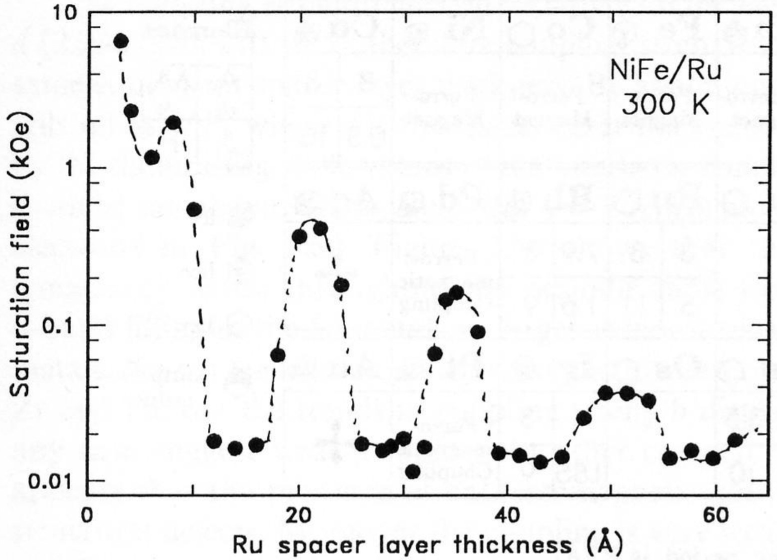

Fig. 2.58. Dependence of saturation field on Ru spacer layer thickness for several series of $Ni_{81}Fe_{19}$/Ru multilayers with structure, 100 Å Ru/[30 Å $Ni_{81}Fe_{19}$/Ru(t_{Ru})]$_{20}$, where the topmost Ru layer thickness is adjusted to be $\simeq 25$ Å for all samples

	$\lvert J_1 \rvert$ at 1st peak (erg/cm^2)	Period (nm)
Cu	0.3	1
V	0.1	0.9
Cr	0.24	1.8
Ir	0.81	0.9
Ru	5.0	1.2

S. S. P. Parkin et al, PRL, 1991.

❖ Modulated magnetic properties in synthetic rare-earth Gd-Y superlattices
Saturation moment, saturation field: oscillatory behavior

J. Kwo et al, PRB **35** 7295 (1987)

Spin-dependent Conduction in Ferromagnetic metals (Two-current model)

First suggested by Mott (1936)
Experimentally confirmed by I. A. Campbell and A. Fert (~1970)

At low temperature
$$\rho = \frac{\rho_{\uparrow}\rho_{\downarrow}}{\rho_{\uparrow} + \rho_{\downarrow}}$$

At high temperature
$$\rho = \frac{\rho_{\uparrow}\rho_{\downarrow} + \rho_{\uparrow\downarrow}(\rho_{\uparrow} + \rho_{\downarrow})}{\rho_{\uparrow} + \rho_{\downarrow} + 4\rho_{\uparrow\downarrow}}$$

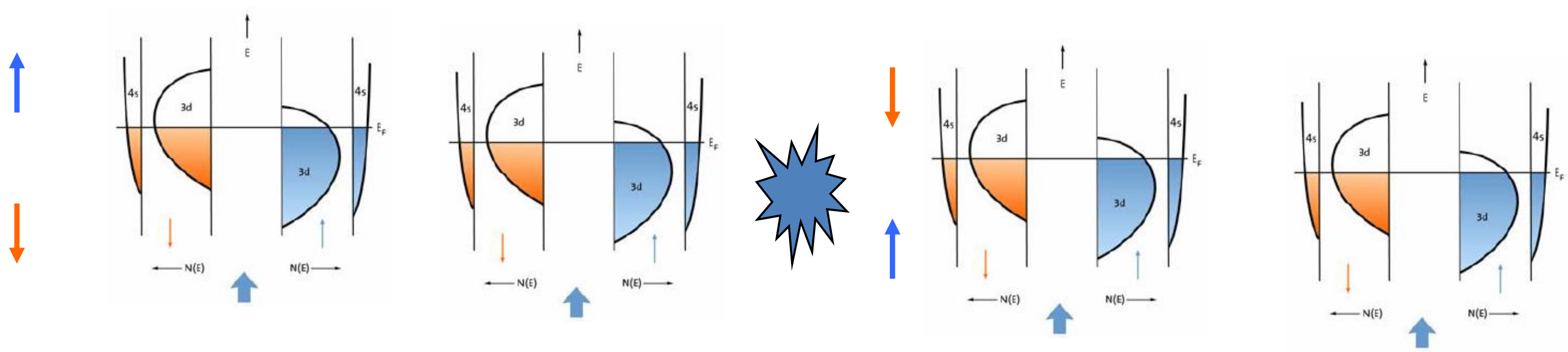

Spin mixing effect equalizes two currents

Two Current Model

***s* electrons carry the electric current**

resistivity (spin-dependent *s* → *d* scattering)

$$R^{S} = \text{const.}\ N_d^{S}$$

number of empty *d* states

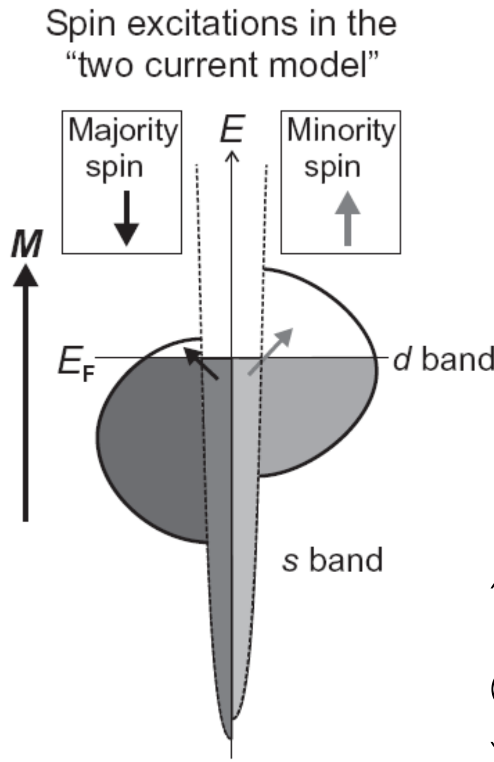

element	N_h^d [a]	$\lvert \boldsymbol{m} \rvert$ [μ_B]	R [b] [Ω m]
Fe (bcc)	3.90	2.216	9.71×10^{-8}
Co (hcp)	2.80	1.715	6.25×10^{-8}
Ni (fcc)	1.75	0.616	6.84×10^{-8}
Cu (fcc)	0.50	–	1.68×10^{-8}

spin selective scattering

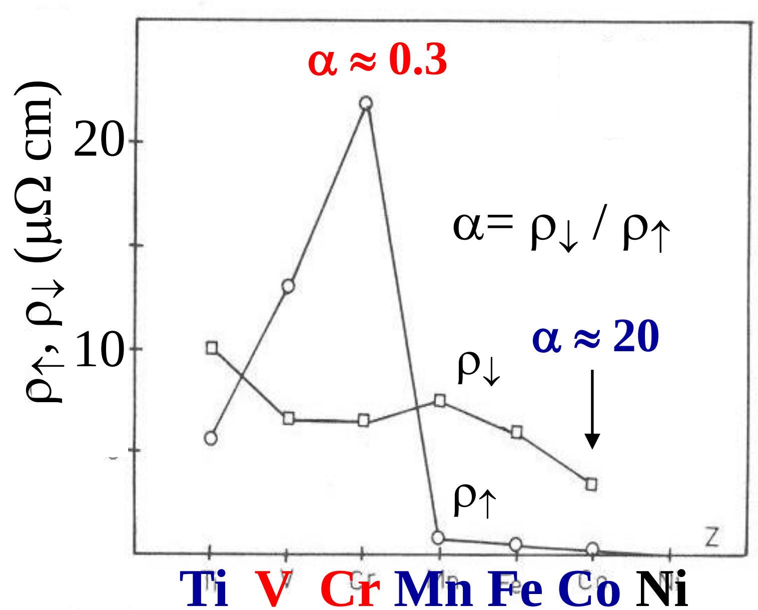

A. Fert, I.A. Campbell, PRL **21**, 1190 (1968)

Anisotropic magnetoresistance (AMR)

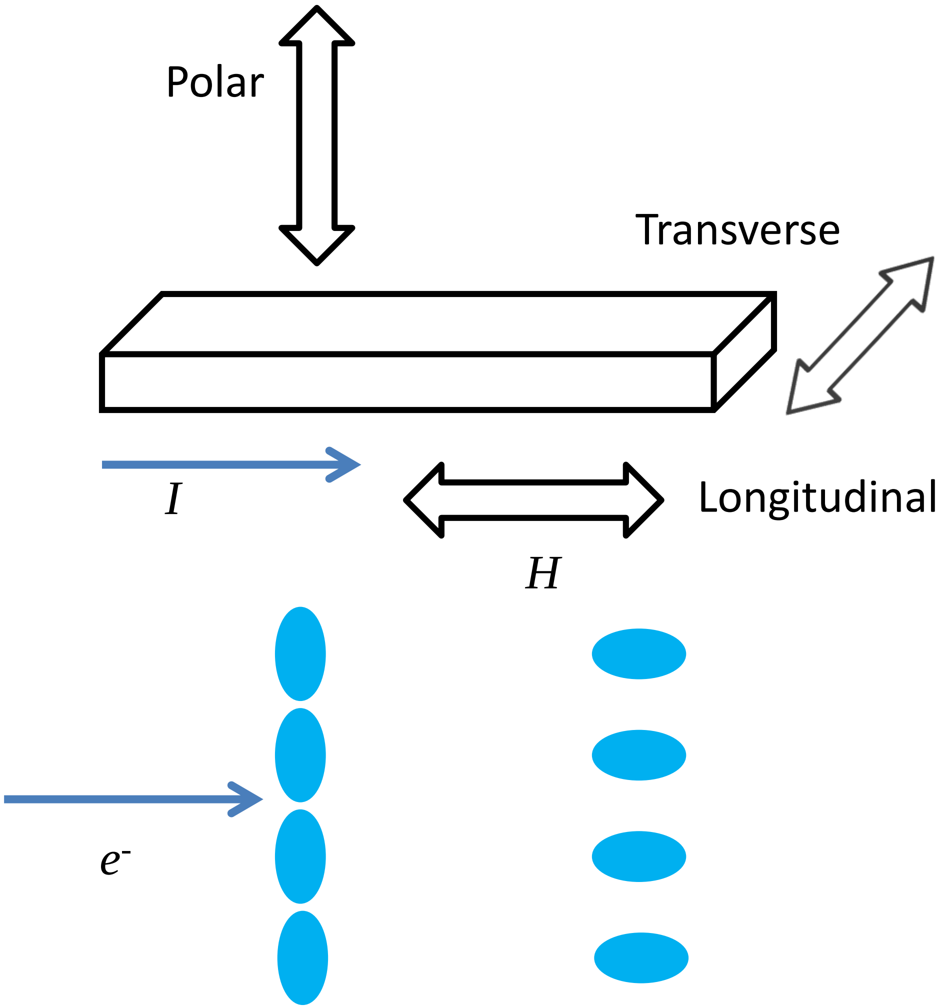

$$R_{Long.} > R_{Trans.}, R_{Pol.}$$

Geometrical size effect

Fe 100nm 10K

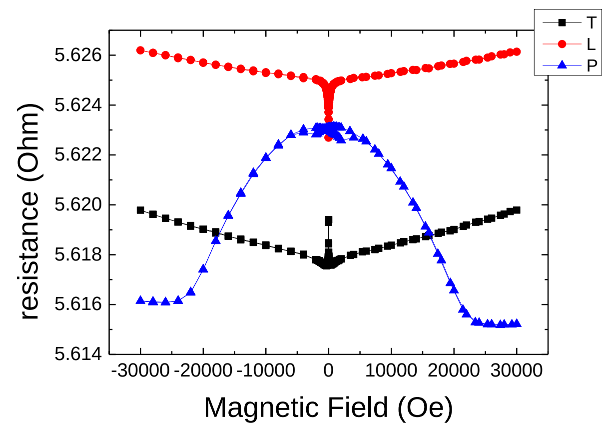

Ni 100nm 10K

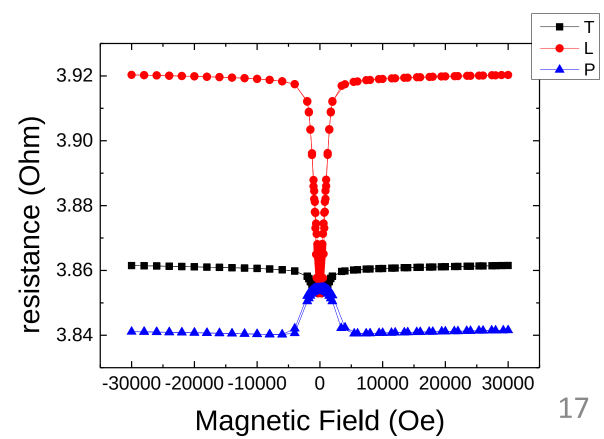

Outline

- Giant Magnetoresistance,
- Tunneling Magnetoresistance
- Spin Transfer Torque
- Pure Spin current (no net charge current)
  - Spin Hall, Inverse Spin Hall effects
  - Spin Pumping effect
  - Spin Seebeck effect
- Micro and nano Magnetics

2007 Nobel prize in Physics

2007年諾貝爾物理獎得主 左 亞伯・費爾(Albert Fert) 與右彼得・葛倫貝格(Peter Grünberg)

(圖片資料來源：Copyright © Nobel Web AB 2007/ Photo: Hans Mehlin)

Giant Magnetoresistance
Tunneling Magnetoresistance

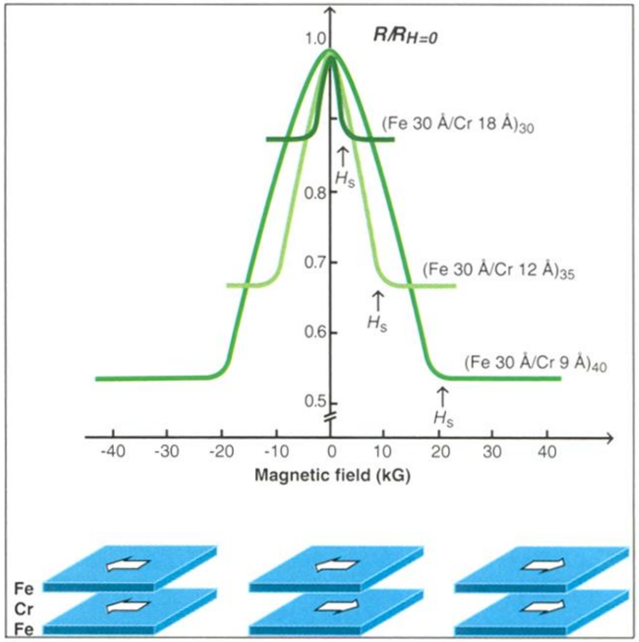

Discovery of Giant MR --
Two-current model combines with magnetic coupling in multilayers

Fert's group, PRL **61**, 2472 (1988)

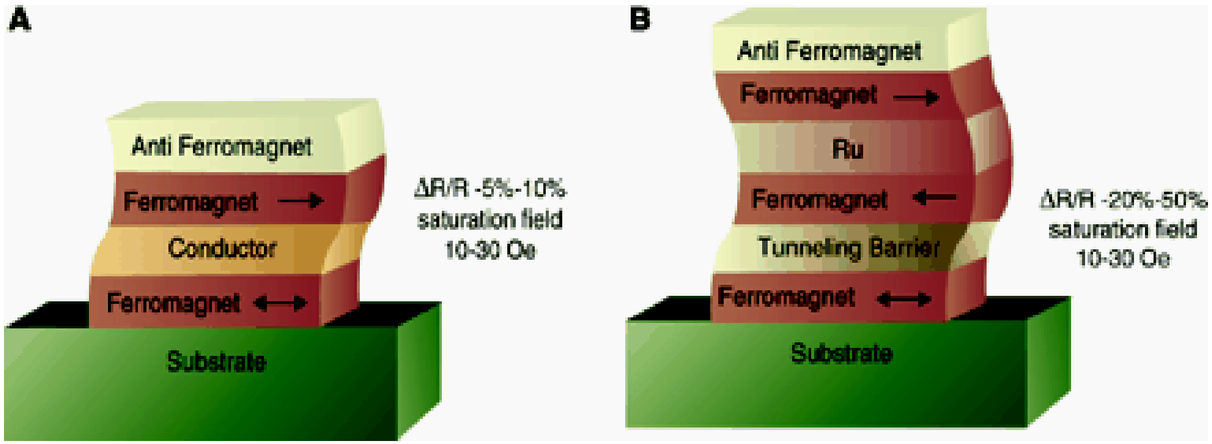

Spin-dependent transport structures.
(A) Spin valve. (B) Magnetic tunnel junction.
(from Science)

Moodera's group, PRL **74**, 3273 (1995)

Miyazaki's group, JMMM **139**, L231(1995)

Spin valve –

a sandwich structure with a free ferromagnetic layer (F) and a fixed F layer pinned by an antiferromagnetic (AF) layer

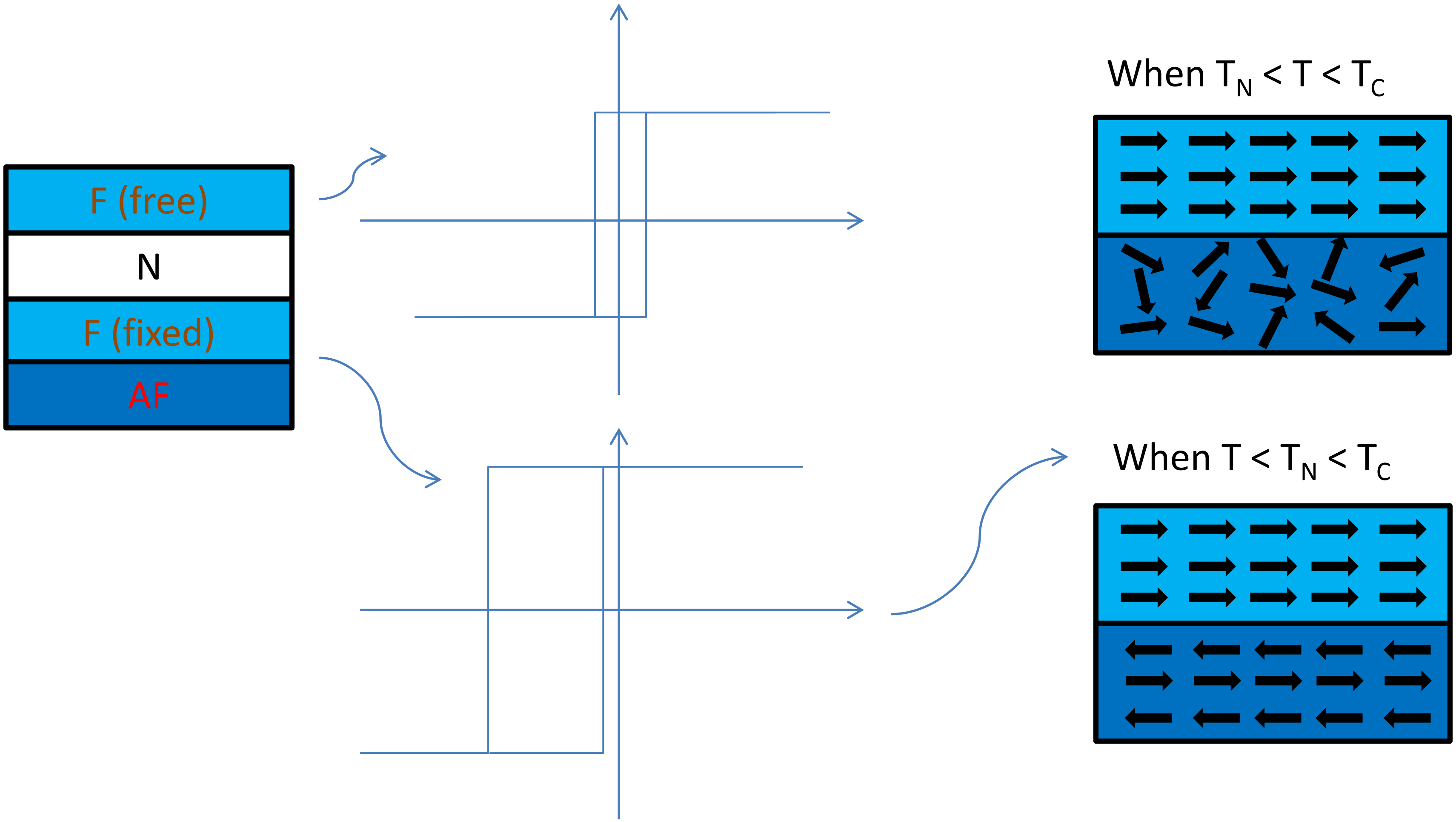

Transport geometry

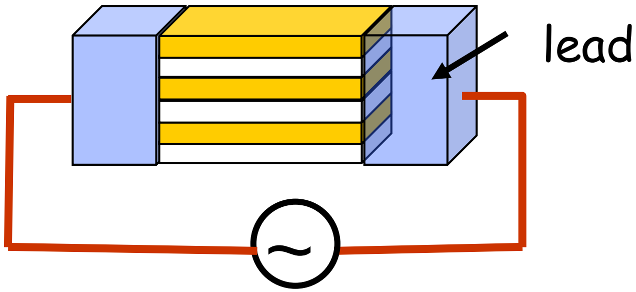

CIP geometry

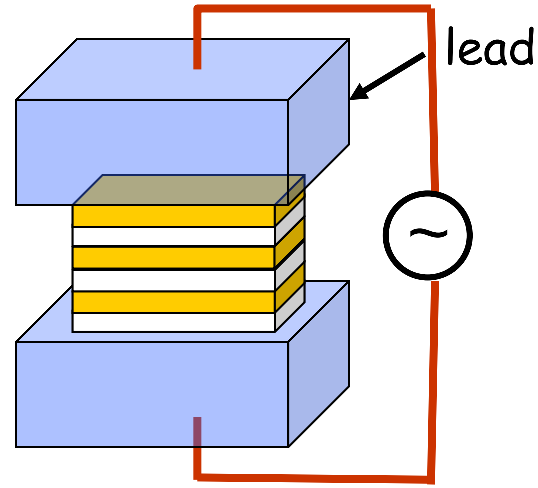

CPP geometry

- In metallic multilayers, CIP resistance can be measured easily.
- CPP resistance needs special techniques.
- From CPP resistance in metallic multilayers, one can measure interface resistances, spin diffusion lengths, and polarization in ferromagnetic materials, etc.
- CPP magnetoresistance of magnetic multilayers: A critical review:

  Jack Bass, Journal of Magnetism and Magnetic Materials 408, 244, (2016).

Valet and Fert model of (CPP-) GMR

Based on the Boltzmann equation

A semi-classical model with spin taken into consideration

$$j_{+(-)} = \frac{1}{e\rho_{+(-)}}\frac{\partial \mu_{+(-)}}{\partial x}$$

$$j_{+} + j_{-} = j_{e}$$

$$\frac{\partial (j_{+} - j_{-})}{\partial x} = \frac{2eN(E_F)\Delta\mu}{\tau_{sf}}$$

$$\frac{\partial^2 \mu_{+(-)}}{\partial z^2} = \frac{\mu_{+(-)}}{l_{sf}^2} \qquad l_{sf}^F = \left[\lambda_{sf}^F / 3(\lambda_{\uparrow}^{-1} + \lambda_{\downarrow}^{-1})\right]^{1/2}, \quad l_{sf}^N = \left[\lambda_{sf}^N \lambda / 6\right]^{1/2}$$

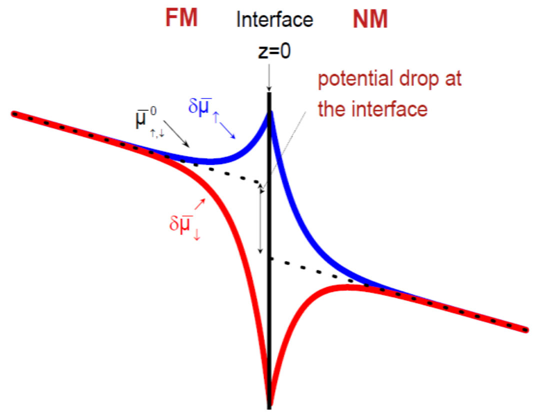

$\Delta\mu$ for antiparallel aligned multilayers

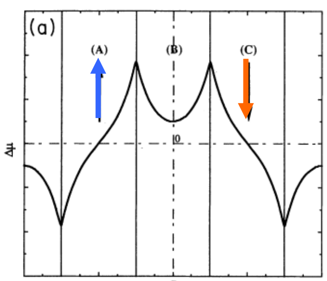

$\Delta\mu$ for parallel aligned multilayers

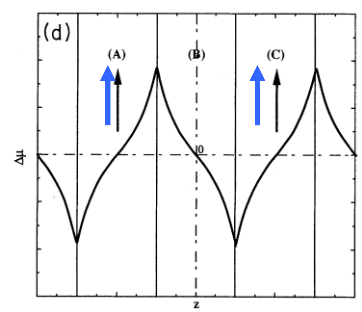

- Spin imbalance induced charge accumulation at the interface is important.
- Spin diffusion length, instead of mean free path, is the dominant physical length scale

Spin Diffusion: The Johnson Transistor non-local measurement

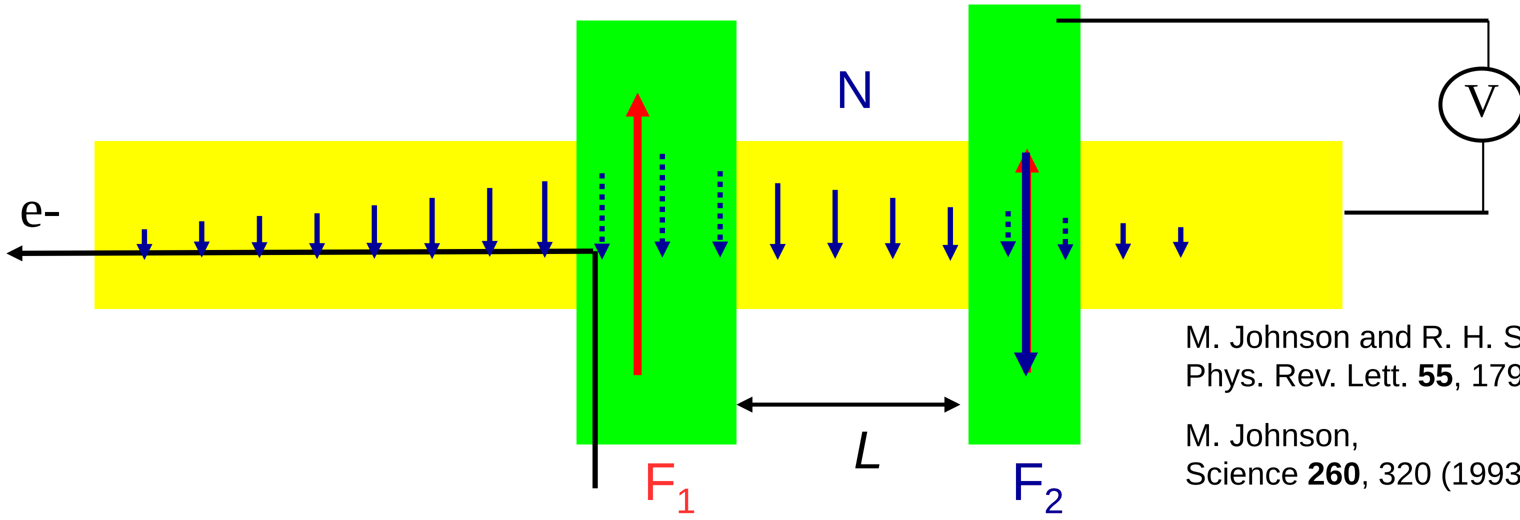

M. Johnson and R. H. Silsbee, Phys. Rev. Lett. **55**, 1790 (1985)

M. Johnson, Science **260**, 320 (1993)

First Experimental Demonstrations

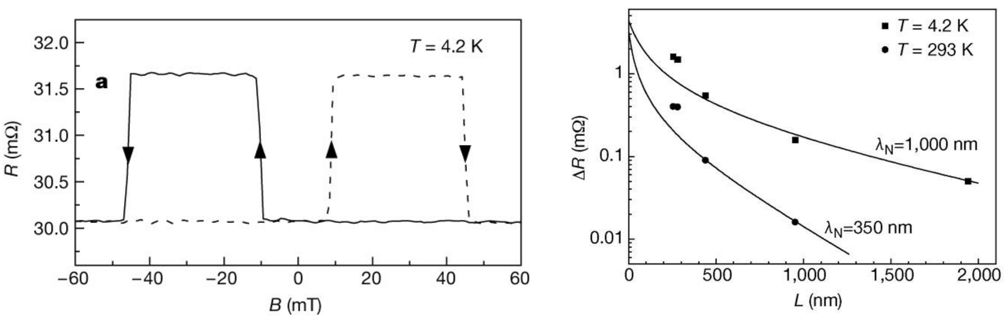

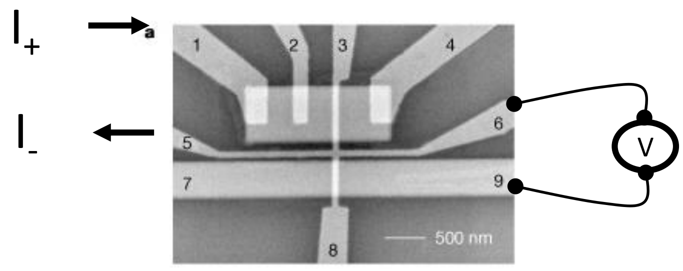

Cu film: λ_s = 1 μm (4.2 K)

Jedema *et al.*, Nature **410**, 345 (2001)